# Characterization of Three *XPG*-Defective Patients Identifies Three Missense Mutations that Impair Repair and Transcription

Annika Schäfer[1], Steffen Schubert[1], Alexei Gratchev[2], Christina Seebode[1], Antje Apel[1], Petra Laspe[1], Lars Hofmann[1], Andreas Ohlenbusch[3], Toshio Mori[4], Nobuhiko Kobayashi[5], Anke Schürer[1], Michael P. Schön[1] and Steffen Emmert[1]

Only 16 *XPG*-defective patients with 20 different mutations have been described. The current hypothesis is that missense mutations impair repair (xeroderma pigmentosum (XP) symptoms), whereas truncating mutations impair both repair and transcription (XP and Cockayne syndrome (CS) symptoms). We identified three cell lines of *XPG*-defective patients (XP40GO, XP72MA, and XP165MA). Patients' fibroblasts showed a reduced post-UVC cell survival. The reduced repair capability, assessed by host cell reactivation, could be complemented by *XPG* cDNA. *XPG* mRNA expression of XP165MA, XP72MA, and XP40GO was 83%, 97%, and 82.5%, respectively, compared with normal fibroblasts. XP165MA was homozygous for a p.G805R mutation; XP72MA and XP40GO were both compound heterozygous (p.W814S and p.E727X, and p.L778P and p.Q150X, respectively). Allele-specific complementation analysis of these five mutations revealed that p.L778P and p.W814S retained considerable residual repair activity. In line with the severe XP/CS phenotypes of XP72MA and XP165MA, even the missense mutations failed to interact with the transcription factor IIH subunits XPD and to some extent cdk7 in coimmunoprecipitation assays. Immunofluorescence techniques revealed that the mutations destabilized early recruitment of XP proteins to localized photodamage and delayed their redistribution *in vivo*. Thus, we identified three *XPG* missense mutations in the I-region of XPG that impaired repair and transcription and resulted in severe XP/CS.

*Journal of Investigative Dermatology* (2013) **133,** 1841–1849; doi:10.1038/jid.2013.54; published online 14 March 2013

## INTRODUCTION

Xeroderma pigmentosum (XP) is caused by a defect in the nucleotide excision repair (NER) pathway. XP is clinically characterized by increased sun sensitivity and freckling within the sun-exposed skin. The skin cancer risk is increased ~1000 fold. XP patients can also exhibit progressive neurological degeneration with features of premature aging (Kraemer *et al.*, 1987). The incidence for XP in Western Europe is estimated at 2.3 per million (Kleijer *et al.*, 2008). XP patients can be assigned to seven complementation groups XPA to XPG depending on the mutated gene (Emmert *et al.*, 2001). In addition, an XP variant form (OMIM: 278750) is caused by mutations in the gene coding for DNA polymerase eta involved in translesion synthesis (Masutani *et al.*, 1999).

The human *XPG* gene (OMIM: 278780) had been mapped to chromosome 13q32.3-q33.1 (Emmert *et al.*, 2001). XPG consists of 1186 amino acids and belongs to the FEN-1 family of structure-specific endonucleases characterized by two highly conserved nuclease domains called N-region and I-region. These regions contain a number of highly conserved acidic residues that are required for the nuclease function (Constantinou *et al.*, 1999; Emmert *et al.*, 2001). The domain between N-region and I-region, ''spacer region'' or ''R-Region'', spans about 600 amino acids, mediates recruitment to NER complexes, and determines substrate specificity (Dunand-Sauthier *et al.*, 2005) (Figure 5a).

In NER, the main function of XPG is the 3′ incision of the damage-containing DNA strand. Further, XPG, independent from its endonuclease activity, is required for the 5′ incision by XPF (OMIM: 278760) (Staresincic *et al.*, 2009). Another important structural role of XPG is required for transcription by stabilizing the architecture of the transcription factor IIH (TFIIH) (Ito *et al.*, 2007).

TFIIH consists of 10 proteins and can be divided into two complexes: The core complex is composed of the six proteins

[1]*Department of Dermatology, Venerology and Allergology, University Medical Center Göttingen, Göttingen, Germany;* [2]*Department of Dermatology, Venerology, and Allergology, University Medical Center Mannheim, Mannheim, Germany;* [3]*Department of Pediatrics, University Medical Center Göttingen, Göttingen, Germany;* [4]*Radioisotope Research Center, Nara Medical University, Kashihara, Nara, Japan and* [5]*Department of Dermatology, Nara Medical University, Kashihara, Nara, Japan*

*Correspondence: Steffen Emmert, Department of Dermatology, Venerology and Allergology, University Medical Center Göttingen, Robert-Koch-Strasse 40, Göttingen 37075, Germany. E-Mail: semmert@gwdg.de*

*Abbreviations: CAK, cdk-activating kinase; CS, Cockayne syndrome; HCR, host cell reactivation; NER, nucleotide excision repair; TFIIH, transcription factor IIH; XP, xeroderma pigmentosum*

*Received 5 July 2012; revised 28 December 2012; accepted 14 January 2013; accepted article preview online 31 January 2013; published online 14 March 2013*

XPB (OMIM: 610651), p62, p52, p44, p32, and p8 trichothiodystrophy. The cdk-activating kinase (CAK) complex contains cdk7, cyclin H, and MAT1. Both complexes are bridged by XPD (OMIM: 278730), which interacts with MAT1 (CAK) and p44 (core). Interactions of the TFIIH proteins XPD, XPB, p62, p44, and cdk7 with XPG have been shown *in vivo* and *in vitro* (Iyer *et al.*, 1996; Thorel *et al.*, 2004; Dunand-Sauthier *et al.*, 2005; Ito *et al.*, 2007).

TFIIH has a dual role: transcription (core complex and CAK) and repair (core complex only). In transcription initiation, the helicase subunit XPB is involved in promoter opening, and the CAK protein cdk7 phosphorylates the C-terminal domain of RNA polymerase II required for promoter escape (Dubaele *et al.*, 2003). Furthermore, cdk7 phosphorylates different nuclear receptors (Le *et al.*, 2010), which, once activated, in turn transactivate transcription of certain genes (Ito *et al.*, 2007). The helicase function of XPD and the ATPase activity of XPB are required for NER (Coin *et al.*, 2007), whereas the activity of CAK is dispensable for this process (Arab *et al.*, 2010).

Consequently, *XPG* mutations have been identified, resulting either in an XP phenotype (repair defect) or in a combined XP/Cockayne syndrome (CS) phenotype (repair and transcriptional defects) (Table 1) (Rapin *et al.*, 2000). Patients suffering from XP/CS exhibit XP symptoms together with classical CS symptoms (OMIM: 216400, 133540) including developmental retardation, dwarfism, and severe neurological abnormalities (Rapin *et al.*, 2000; Emmert *et al.*, 2002).

Within our phenotype–genotype association studies of German NER-defective patients, we identified three human fibroblasts as *XPG* defective and five *XPG* mutations, and showed that truncating and missense mutations impair repair and XPG–TFIIH interaction, resulting in additional transcriptional defects in line with the early-onset severe XP/CS complex phenotype of the patients.

## RESULTS

### Clinical symptoms

Only 16 *XPG*-deficient patients and 20 different *XPG* mutations have been described. We identified and characterized three previously unreported cell lines of *XPG*-deficient patients, XP72MA, XP165MA, and XP40GO. Patients XP72MA and XP165MA were reported as being sun-sensitive since birth and developed freckling within sun-exposed skin as toddlers. Both were diagnosed as severe early-onset XP/CS complex phenotypes. XP72MA developed no skin cancer up to the age of 7 years but exhibited microcephaly, ataxia, and neurological impairment. XP165MA exhibited dwarfism, microcephaly, muscular hypotension, ataxia, reduced muscle proprioceptive reflexes and neurological impairment. This patient died at the age of 2 years from meningitis. Only fibroblast cells but no further clinical data were available from XP40GO.

### Reduced post-UV cell survival

We tested fibroblasts of all patients with respect to their UVC survival with media containing 1 mM caffeine (data not shown) and without caffeine at a density of 5,000 and 7,500 cells per well, respectively. The cells of the patients showed a markedly reduced post-UV cell survival compared with wild-type fibroblasts (Figure 1a).

### Diminished NER capability and XP complementation group G assignment

Host cell reactivation (HCR) using an UV-treated luciferase reporter plasmid revealed reduced NER capability of all three patients' fibroblasts compared with wild-type fibroblasts (Figure 1b). In order to assign the fibroblasts to the XP complementation group G, cotransfection was performed with plasmids expressing wild-type XP cDNA *(XPA–XPG)* along with the reporter gene plasmid. Cotransfection of *XPG* cDNA resulted in enhanced reporter gene activities. Cotransfection of the other XP gene expression plasmids had no effect on luciferase expression (data not shown).

### Normal *XPG* mRNA expression

We measured the *XPG* mRNA expression of the patients' fibroblasts using quantitative real-time reverse-transcriptase–PCR normalized to both housekeeping genes *β-actin* and *GAPDH*. The mean mRNA expression of nine wild-type fibroblasts was set to 100%. XP72MA showed an mRNA expression of 97%, XP40GO of 82.6%, and XP165MA of 83% compared with normal, indicating absence of nonsense-mediated message decay (Supplementary Figure S1 online).

### Previously unreported *XPG* mutations

For *XPG* mutation detection, genomic DNA from primary fibroblasts was sequenced and analyzed following the nomenclature of GenBank accession no. NM_000123.2. Patients XP40GO and XP72MA were both compound heterozygous. In XP40GO, a C to T transition at nucleotide position 891 leads to a change of glutamine at position 150 to a premature stop codon in exon 4. On the other allele, a T to C transition at position 2776 resulted in an amino-acid change from leucine to proline at position 778 in exon 11. In XP72MA, a G to T transversion at nucleotide position 2622 changed glutaminic acid into a stop codon at position 727 in exon 9. On the other allele, tryptophan was changed to serine at position 814 in exon 11 because of a G to C transversion at position 2884. The patient XP165MA was homozygous for a missense mutation in exon 11. A G to A transition at nucleotide position 2856 changed glycine 805 to arginine in exon 11 (Table 1, Figure 5a, Supplementary Figure S2 online).

### Reduced repair activity of the mutated *XPG* alleles

To test the complementation ability of the mutated *XPG* alleles, we constructed allele-specific expression vectors of $XPG_{Q150X}$, $XPG_{E727X}$, $XPG_{G805R}$, $XPG_{L778P}$, and $XPG_{W814S}$ and applied HCR. None of the mutated alleles could complement the NER capability comparable to wild-type pXPG. A considerable residual repair activity was retained with $pXPG_{L778P}$ and $pXPG_{W814S}$, whereas repair activity was greatly reduced with $pXPG_{G805R}$ and the two nonsense mutations $pXPG_{Q150X}$ and $pXPG_{E727X}$ (Figure 2).

**Table 1. Summary of all known *XPG* mutations**

| Protein | Nucleotide | Exon | Phenotype | Patient | References |
|---|---|---|---|---|---|
| p.E11X | c.474G>T | 1 | XP/CS severe, 6 years† | XP20BE het. | Moriwaki *et al.*, 1996; Okinaka *et al.*, 1997 |
| p.Q16X | c.489C>T | 1 | XP/CS severe | XP82DC het. | Emmert *et al.*, 2002 |
| p.L65P | c.637T>C | 2 | Mild XP | XP3HM hom. | Moriwaki *et al.*, 2012 |
| p.P72H | c.658C>A | 2 | XP/CS severe | XPCS4RO het. | Zafeiriou *et al.*, 2001 |
| p.Q136X | c.849C>T | 4 | XP | XP65BE het. | Emmert *et al.*, 2002 |
| p.R138X | c.855C>T | 4 | XP/CS severe, 6 years† | XP20BE het. | Moriwaki *et al.*, 1996; Okinaka *et al.*, 1997 |
| p.Q150X | c. 891 C>T | 4 | — | XP40GO het. | This study |
| p.Q176X | c.969C>T | 5/6 | XP/CS severe | XPCS4RO het. | Zafeiriou *et al.*, 2001 |
| p.E225SfsX19 alternative splicing p.E225-Q231del | Hom. deletion of last nucleotide of splice acceptor site intron 6 | 7 | XP/CS, late onset | XPCS1BD het. | Thorel *et al.*, 2004 |
| p.R263X | c.1230C>T | 7 | XP/CS severe, 20 months† | XPCS2LV het. | Nouspikel *et al.*, 1997 |
| p.L308SfsX12 | c.1364_1365delTC | 7 | XP/CS severe | XP96TA hom. | Emmert *et al.*, 2002 |
| p.R372TfsX6 | c.1557_1560delAGGA | 8 | XP/CS severe, late onset | XP2BI het. | Lalle *et al.*, 2002 |
| p.K498LfsX25 | c.1937delA | 8 | XP/CS severe, late onset | XP3BR.het | Lalle *et al.*, 2002 |
| p.S659VfsX1 | c.2418delA | 9 | XP/CS severe, 6.5 years†, XP/CS severe, 20 months† | XPCS1LV hom. XPCS2LV het. | Nouspikel *et al.*, 1997 |
| p.E727X | c. 2622 G>T | 9 | XP/CS severe | XP72MA het. | This study |
| p.L778P | c. 2776 T>C | 11 | — | XP40GO het. | This study |
| p.A792V | c.2818C>T | 11 | XP mild | XP125LO het. XP124LO het. | Nouspikel and Clarkson, 1994; Norris *et al.*, 1987 |
| p.G805R | c. 2856 G>A | 11 | XP/CS severe, 2 years† | XP165MA hom. | This study |
| p.W814S | c. 2884 G>C | 11 | XP/CS severe | XP72MA het. | This study |
| p.L858P | c.3015C>T | 12 | XP/CS severe, late onset | XP2BI het. | Lalle *et al.*, 2002 |
| p.A874T | c.3063G>A | 12 | XP | XP65BE het. | Emmert *et al.*, 2002 |
| p.V869GfsX11 | c.3049_3050delTG | 12 | XP/CS severe | XP82DC het. | Emmert *et al.*, 2002 |
| p.K917NfsX65 alternative splicing K917fs962-fsX1186 | c.3194delA | 13 | XP/CS severe, late onset | XP3BR het. | Lalle *et al.*, 2002 |
| p.G926AfsX56 | c.3218delT | 13 | XP/CS severe, 7 months† | 94RD27/ XPCS1RO hom. | Nouspikel *et al.*, 1997 |
| p.E960X | c.3321G>T | 13 | XP mild | XP125LO het. XP124LO het. | Nouspikel and Clarkson, 1994; Norris *et al.*, 1987 |
| Not determined | Not determined | | XP mild | XP31KO | Ichihashi *et al.*, 1985 |
| Not determined | Not determined | | XP mild | XP52HM | Yoneda *et al.*, 2007 |

Abbreviations: CS, Cockayne syndrome; het., heterozygous; hom., homozygous; XP, xeroderma pigmentosum.
Mutations are listed in order of their appearance on the gene from 5′ to 3′ (based on GenBank accession no. NM_000123.2).
†Age at death.

**All five *XPG* mutations impair interaction with TFIIH subunits**

To test how the *XPG* mutations affect the interaction of XPG with TFIIH, we constructed C-terminal mycHis-tagged XPG allele–specific expression vectors. HEK932A cells were transfected with plasmids expressing either $XPG_{wt}$mycHis or $XPG_{mut}$mycHis. Immunoprecipitation probes (anti-myc) were subjected to immunoblot analysis against XPD and cdk7. Both proteins XPD and cdk7 were coimmunoprecipitated with $XPG_{wt}$mycHis under physiological conditions of 150 mM NaCl. We found in three independent experiments repeatedly that coimmunoprecipitation of XPD and cdk7 protein was not observed or diminished with all five $XPG_{mut}$mycHis constructs including the three missense mutations (Figure 3).

**No recruitment of XPG protein to sites of local DNA damage in *XPG*-deficient cells**

To assess how the *XPG* mutations affect the assembly of the NER proteins, we performed time-course experiments for protein recruitment to DNA photodamage, as well as release from photodamage 6 minutes, 15 minutes, 30 minutes,

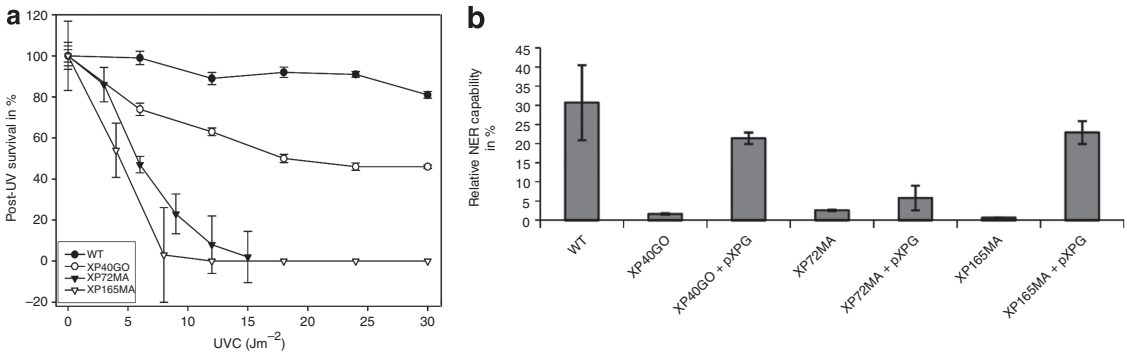


**Figure 1. Functional repair assays and XPG assignment.** (**a**) Reduced post-UV cell survival of patients' fibroblasts and control cells. A total of $5 \times 103$ cells were seeded in quadruplicates in 96-well plates and irradiated with increasing doses of UVC (0–30 J m$^{-2}$). Cell survival was determined through an MTT assay, and survival of nonirradiated cells was set to 100%. (**b**) Reduced repair capability of patients' fibroblasts and assignment to XPG. Cells were transfected with either 250 J m$^{-2}$ UV-irradiated or nonirradiated firefly luciferase reporter gene plasmids. The repair capacity of fibroblasts is reflected by the reactivation of luciferase enzyme expression from the irradiated versus nonirradiated plasmids. Simultaneous cotransfection of an XPG cDNA-containing plasmid complemented the repair defect in the cells. Data are presented as the mean ± SD. At least triplicate experiments were performed. NER, nucleotide excision repair; WT, wild type.

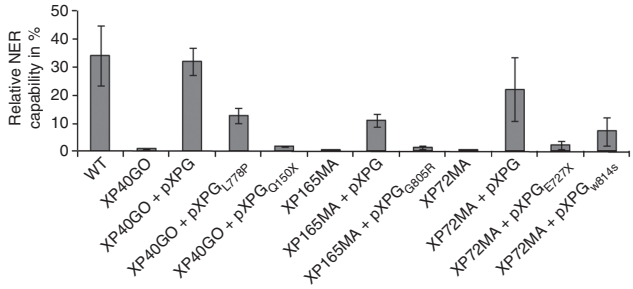


**Figure 2. Complementation ability of the *XPG* mutations.** Allele-specific XPG expression vectors were generated by site-directed mutagenesis for all five mutations. Host cell reactivation (HCR) was used and wild-type XPG as well as mutated XPG expression vectors were cotransfected along with the luciferase reporter gene plasmid. Repair capability is depicted as percentage of luciferase expression (irradiated vs. unirradiated pcmvLUC). At least $n = 6$ transfections were performed. Data are presented as mean ± SD. NER, nucleotide excision repair; WT, wild type.

3 hours, 6 hours, and 24 hours after UV irradiation in our three *XPG*-deficient cells compared with wild-type and XP3BR *XPG*-deficient control fibroblasts using immunofluorescence (Supplementary Figure S3 online). An XPG fluorescence staining in wild-type cells revealed rapid recruitment and redistribution of XPG protein to and from photodamage (Figure 4e). In contrast, no positive XPG staining in cell nuclei was observed in the fibroblasts of all three patients and the *XPG*-deficient control at any time point after UV irradiation. As the applied XPG antibody 8H7 maps to the C-terminal region of XPG, the truncated proteins $XPG_{Q150X}$ in XP40GO and $XPG_{E727X}$ in XP72MA, cannot, most likely, be recognized.

### Early recruitment of other XP proteins is selectively delayed in *XPG*-deficient cells

Immediately (6 minutes) after UV irradiation, all fibroblasts (wild-type and *XPG*-deficient) were stained positive for cyclobutane pyrimidine dimers and pryrimidine-6,4-pyrimidone photoproducts as expected. We found that XPA (OMIM: 278700) was equally rapidly recruited in wild-type, as well as in all *XPG*-deficient fibroblasts XP40GO, XP165MA, XP72MA, and XP3BR (50%, 46%, 36%, and 38%, respectively) (Figure 4a). There was a markedly reduced and delayed XPB recruitment in XP72MA (1%) (Figure 4b). In XP40GO and XP72MA cells, early XPC (OMIM: 278720) recruitment was clearly delayed (7 and 4%) (Figure 4c). ERCC1 (complexed with XPF; OMIM: 126380) protein recruitment was delayed in all three *XPG*-deficient cells compared with wild type and XP3BR (Figure 4d).

### No redistribution of other XP proteins in all *XPG*-deficient cells

Thirty minutes after UV irradiation, the *XPG*-deficient cells reached their maximum of XP protein recruitment to photodamage (range: 39–60%). All XP proteins tested (XPC, XPB, XPA, and ERCC1) were recruited to sites of local photodamage. At this time point, wild-type cells already released nearly all XP proteins from DNA lesions (range: 2–9%, Figure 4). After 24 hours, redistribution of XP proteins also started in *XPG*-deficient cells; however, a considerable amount of XP proteins persisted in the cells of all patients and XP3BR control cells at sites of local photodamage (range: 13–49%). This paralleled a defective DNA photoproduct removal in all *XPG*-deficient cells for 6,4PPs, as well as for CPD (Figure 4f and g). Nevertheless, all *XPG*-deficient cells could remove 50–70% of their 6,4PP within 24 hours but no CPD (Figure 4g).

## DISCUSSION

### *XPG* mutations

To date, only 16 patients have been assigned to the complementation group G. Six of these patients developed classical XP symptoms. The other 10 patients exhibited the XP/CS complex phenotype (Table 1). Our patients' phenotypes are in good agreement with previous clinical reports of XP/CS complex patients (Moriwaki *et al.*, 1996; Emmert *et al.*, 2002).

So far, only 20 *XPG* mutations have been reported (Table 1). In general, the presence of one missense mutation retaining some functional XPG activity confers milder XP symptoms (Emmert *et al.*, 2002). For example, the p.A792V missense

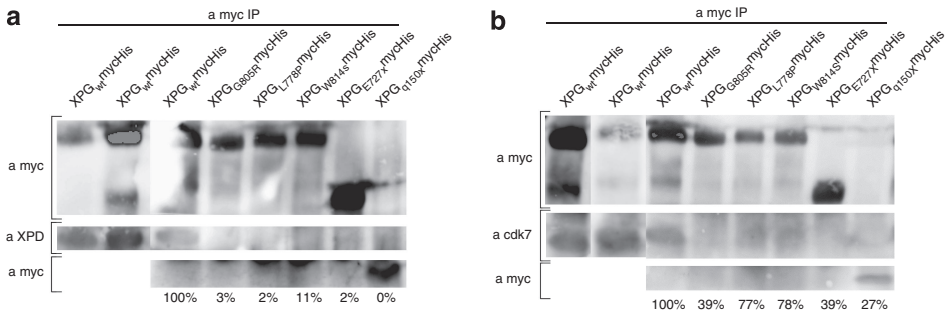


**Figure 3. *XPG* mutations impair interaction with TFIIH subunits XPD and cdk7.** Wild-type XPG$_{wt}$mycHis and XPG$_{mut}$mycHis constructs were expressed in HEK293A cells. Whole-cell extracts were used for immunoprecipitation with anti-myc antibody, and purified complexes were analyzed by immunoblotting with the antibodies indicated. (**a**) No interaction with XPD was observed with all five XPG$_{mut}$mycHis proteins in contrast to XPG$_{wt}$mycHis. (**b**) No or reduced amounts of cdk7 were coimmunoprecipitated with all five XPG$_{mut}$mycHis proteins. The numbers indicate the ratio of band intensities for XPD and cdk7 obtained with each mutated *XPG* construct relative to those obtained with the wild-type XPG construct (in %). Identical results were found in three independent experiments.

mutation is also located in the I-region but resulted just in a mild XP phenotype without any neurological abnormalities in patients with XP124LO and XP125LO (Nouspikel and Clarkson, 1994). Two missense mutations have already been described that do not fit into this hypothesis. The mutation p.P72H is located in the N-region, resulted in a severe early-onset XP/CS complex phenotype in XPCS4RO (Zafeiriou *et al.*, 2001), and was predicted to greatly destabilize the XPG protein (Thorel *et al.*, 2004). The mutation p.L858P described in XP2BI is located in the same I-region as our missense mutations, but it resulted in a mild late-onset XP/CS phenotype probably because of some retained transcriptional activity (Lalle *et al.*, 2002). On the basis of the clinical descriptions and the immunoprecipitation results (Figure 3), our missense mutations in the I-region may more profoundly impair the transcriptional role of XPG compared with p.L858P.

Highly conserved amino-acid residues in the I-region and the N-region are necessary for endonuclease proficiency of XPG (Hosfield *et al.*, 1998; Constantinou *et al.*, 1999). An alignment of the I-region (Figure 5b) revealed that the mutated amino-acid residues L778, G805, and W814 are highly conserved in humans, mice, and chickens. L778 is also highly conserved through different members of the FEN-1 nuclease family (Constantinou *et al.*, 1999). W814 is adjacent to the highly conserved amino-acid residue D812, which is crucial for XPG cleavage activity (Constantinou *et al.*, 1999). This is in accordance with our results and can readily explain the diminished repair capability of the patients' fibroblasts.

### Mutations impair interaction with TFIIH

That the truncated XPG proteins XPG$_{Q150X}$mycHis (XP40GO) and XPG$_{E727X}$mycHis (XP72MA) showed no interaction with XPD or with cdk7 is in line with previous reports (Ito *et al.*, 2007; Arab *et al.*, 2010). Our three missense mutations were all located within the I-region of XPG (747–928), which was shown to interact with XPD. Two XPG–XPD-binding regions were identified *in vitro*: XPG$_{1–377}$ and XPG$_{747–928}$. In addition, single amino-acid residues in XPG are also crucial for other XPG-protein interactions (Iyer *et al.*, 1996). For example, Arg992 is crucial for PCNA protein binding (Gary *et al.*, 1997). This supports our findings that missense mutations impair XPG-protein interactions in general and that the single amino-acid residues L778, G805, and W814 in XPG are crucial for XPG–XPD interaction in particular. Therefore, the severe early-onset XP/CS complex phenotype of our patients with XP165MA and XP72MA can be explained by impaired XPG–XPD, and to a lesser extent XPG–cdk7, interactions due to the truncating and the three *XPG* missense mutations. Ito *et al.* (2007) suggested that XPG and XPD cooperatively mediate the anchoring of CAK to core TFIIH. Core TFIIH is involved in NER, whereas CAK is dispensable (Arab *et al.*, 2010). However, CAK activity as part of TFIIH is involved in general transcription (Ito *et al.*, 2007; Scharer, 2008; Arab *et al.*, 2010; Le *et al.*, 2010). Abnormalities in the transcriptional process in addition to defective repair cause CS features in XP-mutated patients (Ito *et al.*, 2007; Arab *et al.*, 2010). On the basis of our findings and the proposed functional consequences, we can reasonably assume that XP40GO also suffered from a severe XP/CS complex phenotype.

### Mutation-specific effects on repair factor assembly

*In vitro* and *in vivo* investigations suggest a sequential assembly of the NER factors (Volker *et al.*, 2001; Riedl *et al.*, 2003). That XPG was not recruited to local photodamage indicates that all five mutated XPG proteins do not properly interact with other NER proteins. Oh *et al.* (2007) also described an impaired recruitment of XPG in *XPG*-deficient cells. We also found recruitment of XPC, XPB, XPA, and ERCC1 (complexed with XPF) proteins to local photodamage in all *XPG*-deficient cells at 30 minutes after UV irradiation in line with previous reports on *XPG*-deficient cells with other mutations (Thorel *et al.*, 2004; Oh *et al.*, 2007; Arab *et al.*, 2010). At a very early time point (6 minutes), XPA was also normally fast recruited, indicating that XPG is dispensable for XPA recruitment (Oh *et al.*, 2007). However, the early fast recruitment of XPB and XPC may depend on specific *XPG* mutations. We found a delayed early recruitment of XPC in XP72MA and XP40GO and of XPB in XP72MA. This might reflect that the strong functional interaction between XPC and TFIIH (Araujo *et al.*, 2001) is also affected by the

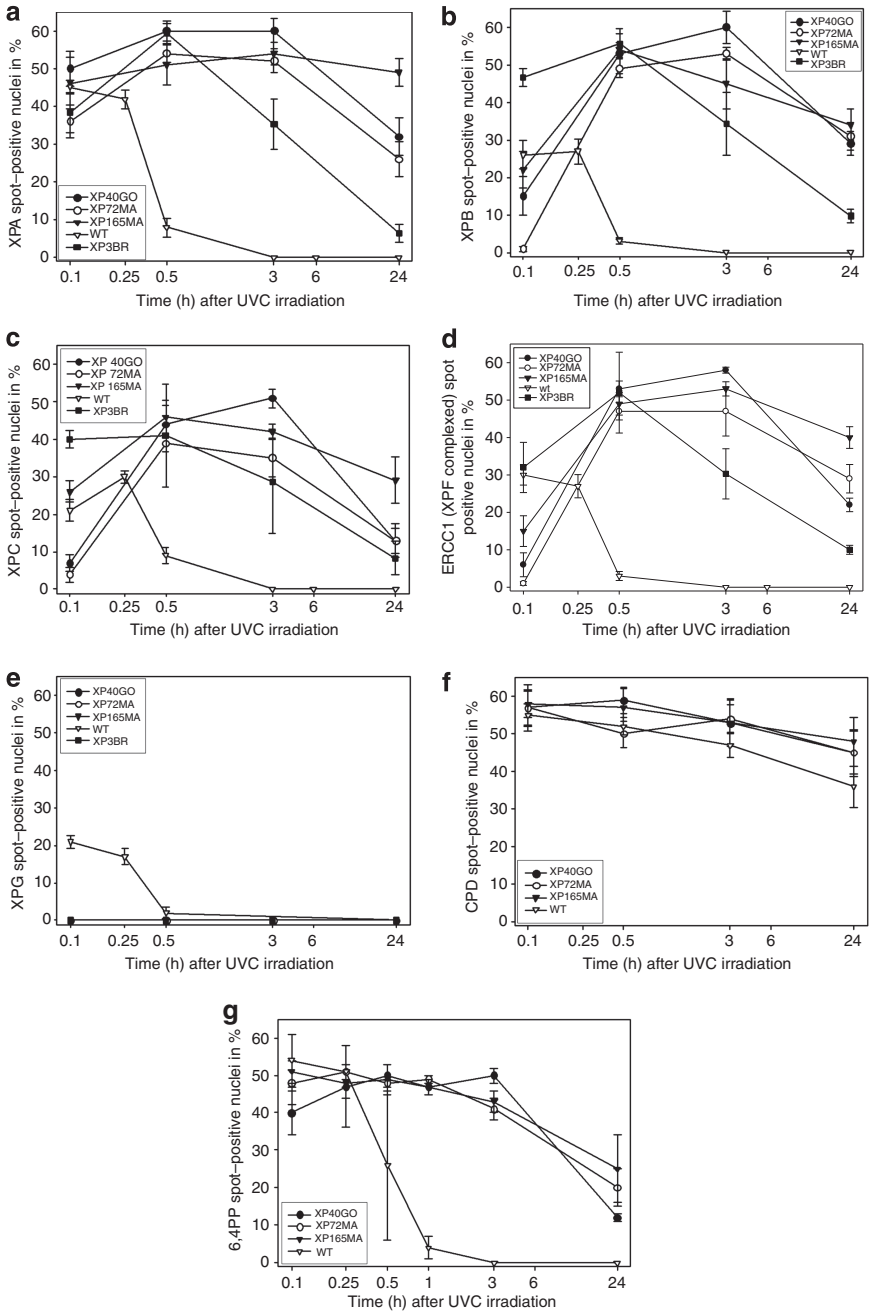


**Figure 4. Selectively delayed early recruitment and impaired redistribution of xeroderma pigmentosum (XP) proteins in *XPG*-deficient fibroblasts.** The *XPG*-deficient cell line XP3BR was used as a control in addition to wild-type (WT) cells, because the cells harbor compound heterozygous deletions of one nucleotide each (c.1937delA and c.3194delA); however, because of a minor splice variant, this cell still retains an almost full-length XP protein of 1,185, instead of 1,186 amino acids (p.K917fs962-fsX1186). The time course of XP protein recruitment and redistribution after local UV irradiation was assessed with immunofluorescence. Patients' and wild-type fibroblasts were irradiated with 100 J m$^{-2}$ and incubated for the different intervals (0.1 hours, 0.5 hours, 3 hours, 6 hours, and 24 hours). Cells were fixed, permeabilized, and stained with antibodies against either one of the XP proteins (**a**) XPA, (**b**) XPB, (**c**) XPC, (**d**) ERCC1, (**e**) XPG, or one of the UV lesions (**f**) CPD and (**g**) 6,4PP. A minimum of 100 nuclei were assessed at each time point to calculate the percentage of positively stained nuclei. Data are presented as mean ± SD.

destabilization of TFIIH because of impaired interactions with XPG (Ito *et al.*, 2007; Arab *et al.*, 2010). ERCC1–XPF recruitment depends on XPG (Riedl *et al.*, 2003). In line with that, we observed a delayed early recruitment of ERCCI in all three *XPG*-deficient cells (Figure 4). In the XP3BR controls, early XP recruitment was normal, which may be explained by a normal-length *XPG* splice variant in this cell line (Lalle *et al.*, 2002).

Redistribution of XP proteins results from the proceeding repair of DNA photoproducts (Dunand-Sauthier *et al.*, 2005; Oh *et al.*, 2007). Defective NER was reflected in all of our *XPG*-deficient cells by persistence of XPA, XPB, XPC, and

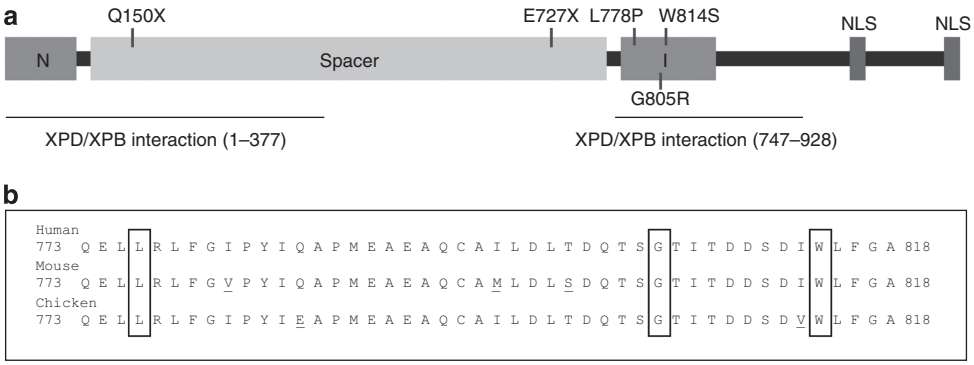


**Figure 5. The XPG protein.** (**a**) Scheme of the wild-type XPG protein with N-region (1–95) and I-region (766–873) corresponding to the endonuclease function, as well as C-terminal nuclear localization signals (NLS). The spacer region is located between the N-region and I-region, and spans about 600 amino acids. The five XPG-protein alterations are depicted. XPB and XPD interaction sites (1–377 and 747–928) are underlined. (**b**) Alignment of a stretch of the I-region (human amino acids 773–818) over different species (human, mouse, and chicken) revealed the three amino-acid residues L778, G805, and W814 to be highly conserved. Affected amino acids are framed. Underlined amino acids differ between the species.

ERCC1 proteins at local photodamage even after 24 hours (Figure 4). The least persistence was observed in XP3BR, again, probably because of a normal-length *XPG* splice variant. This is in agreement with observations from Arab *et al.* (2010) and Oh *et al.* (2007) for cells from other XPG/CS patients, and this has also been demonstrated for cells from XPA, XPB, and XPC patients (Riedl *et al.*, 2003; Oh *et al.*, 2007), as well as from XPD patients with and without neurological symptoms (Boyle *et al.*, 2008). This indicates that the impaired redistribution of XP proteins reflects impaired repair related to a XP phenotype and not to XP/CS complex or XP plus neurological symptoms phenotypes. That there was removal of 6-4PP over 24 hours in all cells (Figure 4g) is in line with the residual repair activity of the cells assessed by HCR (Figure 1b), as well as by testing each mutated allele (Figure 2), and in good agreement with previous reports (Emmert *et al.*, 2002).

## MATERIALS AND METHODS

### Cells and cell-culture conditions

XP40GO (XP30MA), XP72MA, and XP165MA *XPG*-deficient primary human fibroblasts and clinical data for XP72MA and XP165MA were collected at the Department of Dermatology in Mannheim. XP3BR fibroblasts were obtained from the Coriell Institute, Camden, NJ. Wild-type primary fibroblasts (wt1GO-wt9GO) were established in Göttingen. HEK293A cells were purchased from Invitrogen (Karlsruhe, Germany). All cells were cultured in Dulbecco's modified Eagle's medium (Invitrogen) supplemented with 2% glutamine and 10% fetal bovine serum from Biochrom (Berlin, Germany). All studies were conducted according to the Declaration of Helsinki principles. The studies were performed in accordance with protocols approved by the University of Göttingen Institutional Review Board.

### Post-UV cell survival

The post-UV cell survival was assessed as described (Thoms *et al.*, 2011). The mean absorption value of the nonirradiated cells was set to 100% survival to calculate the relative post-UV survival of the irradiated cells. At least two independent experiments were performed in quadruplicate.

### Plasmid HCR and complementation group assignment

Plasmid HCR and complementation group assignment were performed as described previously (Emmert *et al.*, 2002, 2006). The plasmids were a generous gift from M. Hedayati and late L. Grossman (Johns Hopkins University, Baltimore, MD) and K.H. Kraemer (NCI, Bethesda, MD). At least triplicate experiments were performed.

### Genomic *XPG* DNA sequencing

Genomic DNA was isolated using a QIAamp DNA Blood Mini Kit (Qiagen, Hilden, Germany). Primer pairs for amplification of the entire coding region and all exon/intron boundaries are listed in Supplementary Table S1 online. DNA sequencing was performed using a BigDyeTerminator v3.1 Cycle Sequencing Kit (Applied Biosystems, Foster City, CA) and analyzed with a 3100-Avant Genetic Analyzer (Applied Biosystems) and Chromas Lite version 2.01 software (Technelysium Pty, Brisbane, Australia).

### *XPG* mRNA expression analysis

Total RNA was isolated using an RNeasy Mini Kit and an RNase-free DNase Set (Qiagen). cDNA was generated using a RevertAid H Minus First strand cDNA synthesis Kit (MBI Fermentas, St Leon-Rot, Germany). Expression levels of *XPG* cDNA were determined by quantitative real-time PCR using a QuantiTect SYBR Green Kit (Qiagen). The expression of *GAPDH* and *β-actin* mRNA was measured as reference. All primers were purchased from Qiagen (QuantiTect Primer Assays; Cat. No.: QT00029246, QT00079247, and QT00095431, respectively). Standards were generated by spectrophotometric quantification of specific PCR products, and dilution series ranging from 500 to 0.0005 amoles were used in each run. The *XPG* mRNA levels were normalized to the levels of both reference genes (*β-actin* and *GAPDH).* For calculation of the *XPG* mRNA expression of the three patients, the mean *XPG* mRNA expression level of nine wild-type fibroblasts was set to 100%.

### Generation of pXPG$_{mut}$ and myc-tagged XPG$_{wt}$mycHis and XPG$_{mut}$mycHis constructs

To test the repair function of the *XPG* mutations, site-directed mutagenesis was applied to pXPG (primer sequences summarized in Supplementary Table S2 online), and HCR was performed as

described (Emmert *et al.*, 2002). Wild-type *XPG* cDNA was amplified from pXPG plasmid with forward primer 5′-AATGCGGCCGCTTAGAGTAGAAGTTGTCG-3′ and reverse primer 5′-ATTGGTACCGGTTTTCCTTTTTCTTCC-3′, each carrying a *Not*I or *Kpn*I restriction site, respectively, and subcloned into pcDNA3.1/myc-His(−)A. For generation of the two truncated proteins, $XPG_{1–150}$mycHis and $XPG_{1–727}$mycHis, the forward primer 5′-AATGCGGCCGCTTAGAGTAGAAGTTGTCG-3′ was used together with the reverse primers 5′-ATTGGTACCTTGTAAAGGAGGCAAAAC-3′ and 5′-ATTGGTACCTTCATGGAGCGAATCTTCCGC-3′, respectively. For the $XPG_{mut}$mycHis constructs carrying one of the three missense mutations, $XPG_{wt}$mycHis was used as a template for site-directed mutagenesis as described above (Supplementary Table S2 online).

### Immunoprecipitation

For immunoprecipitation of the mycHis-tagged XPG proteins, HEK293A cells were used. Twenty-four hours after transfection, cells were trypsinized and diluted in 1 ml of IP Lysis Buffer (50 mM Tris–HCl (pH 7.6 at 4 °C), 150 mM NaCl, 1 mM DTT, and 1 mM EDTA) containing 1 mM phenylmethylsulfonyl fluoride and protease inhibitor (Complete ULTRA Tablets Mini EDTA free EASYpack; Roche, Mannheim, Germany). Precipitation of $XPG_{mycHis}$ protein was performed by adding an anti-myc mouse antibody at a dilution of 1:1,000 (Cell Signaling, Danvers, MA). Control IP was performed using a mouse IgG antibody (Dako, Glostrup, Denmark). A volume of 50 µl of a 1:1 mixture of AgaroseA beads and AgaroseG+ (Santa Cruz Biotechnology, Santa Cruz, CA) was added to each sample and washed five times with IP Lysis Buffer.

### Horizontal SDS-PAGE and western blotting

For SDS-PAGE, the Amersham ECL electrophoresis system with a precast 4–12% polyacrylamide gradient gel (Amersham, GE Healthcare Biosciences, Piscataway, NJ) was used applying the wet-blot method in a XCellII Blot Module (Invitrogen). As blocking buffer for anti-myc and anti-cdk7 mouse antibodies (myc 9B11 and cdk7 MOI; Cell Signaling Technology), Tris-buffered saline (20 mM Tris-HCl, pH 7.5, and 150 mM NaCl) containing 0.1% Tween and 5% milk powder (Merck, Darmstadt, Germany) was used. Blocking buffer for the anti-XPD rabbit antibody (H-150; Santa Cruz Biotechnology) was obtained from the WesternBreeze Chemiluminescent Immunodetection System (Invitrogen). Incubation with the specific antibodies was performed over night at 4 °C (anti-myc ab 1:1,000, anti-cdk7 ab 1:1,000, and anti-XPD ab 1:100). Finally, incubation with the secondary antibodies (anti-mouse or anti-rabbit) and chemiluminescent substrates was performed using the WesternBreeze Chemiluminescent Immunodetection Systems and analyzed using the luminescent image analyzer LAS-4000 (Fujifilm, Düsseldorf, Deutschland).

### Immunofluorescence XP protein recruitment kinetics

Fibroblast cells ($2 \times 10^4$ per well) were seeded on glass coverslips in 24-well plates (Greiner Bio-One, Frickenhausen, Germany) and irradiated with 100 J m$^{-2}$ UVC (UVC 500 UV Crosslinker; AmershamBiosciences, Freiburg, Germany) through a 5-µm Isopore polycarbonate filter membrane (Neuro Probe Inc., Gaithersburg, MD). At different time points (6 minuntes, 15 minuntes, 30 minuntes, 3 hours, 6 hours, and 24 hours), cells were fixed with 3.7% formaldehyde and permeabilized with 0.1% Triton-X-100 (Merck). Antibodies against one of the XP proteins (XPA, FL-273; XPB, S-19; XPC, H-300; ERCC1, FL-297; and XPG, 8H7; Santa Cruz Biotechnology) were added (1:50), followed by incubation with a secondary anti-rabbit antibody conjugated with DyLight488 (1:400) (Dianova, Hamburg, Germany). For detection of photolesions, DNA was denatured with 2 M HCl before addition of CPD (1:1,000) or with 6,4PP antibodies (1:500; 30 minutes at 37 °C), followed by incubation with a secondary anti-mouse antibody conjugated with Dylight594 for 1 hours at 37 °C (1:500) (Dianova). Cells were mounted with the Vectashield Mounting Medium for 4′,6-diamidino-2-phenylindole fluorecsence (Vector Laboratories, Inc., Burlingame, Canada), and digital images were taken with an Axio Imager.M1 microscope (Carl Zeiss, Oberkochen, Germany). At least 100 nuclei were evaluated for the calculation of percentage of positive staining.

## CONFLICT OF INTEREST

The authors state no conflict of interest.

## ACKNOWLEDGMENTS

This work was supported by a grant from the German Cancer Aid (Deutsche Krebshilfe e.V.; no.: 108616) to AS, PL, and SE, and in part by the Deutsche Forschungsgemeinschaft DFG (GRK 1034) to SS and SE, as well as the Research Program, Faculty of Medicine, Georg-August-University Göttingen, to AS and SE. We also thank Professor E.G. Jung for the work and support.

## SUPPLEMENTARY MATERIAL

Supplementary material is linked to the online version of the paper at http://www.nature.com/jid

## REFERENCES

Arab HH, Wani G, Ray A *et al.* (2010) Dissociation of CAK from core TFIIH reveals a functional link between XP-G/CS and the TFIIH disassembly state. *PLoS One* 5:e11007

Araujo SJ, Nigg EA, Wood RD (2001) Strong functional interactions of TFIIH with XPC and XPG in human DNA nucleotide excision repair, without a preassembled repairosome. *Mol Cell Biol* 21:2281–91

Boyle J, Ueda T, Oh KS *et al.* (2008) Persistence of repair proteins at unrepaired DNA damage distinguishes diseases with ERCC2 (XPD) mutations: cancer-prone xeroderma pigmentosum vs. non-cancer-prone trichothiodystrophy. *Hum Mutat* 29:1194–208

Coin F, Oksenych V, Egly JM (2007) Distinct roles for the XPB/p52 and XPD/p44 subcomplexes of TFIIH in damaged DNA opening during nucleotide excision repair. *Mol Cell* 26:245–56

Constantinou A, Gunz D, Evans E *et al.* (1999) Conserved residues of human XPG protein important for nuclease activity and function in nucleotide excision repair. *J Biol Chem* 274:5637–48

Dubaele S, Proietti DeSL, Bienstock RJ *et al.* (2003) Basal transcription defect discriminates between xeroderma pigmentosum and trichothiodystrophy in XPD patients. *Mol Cell* 11:1635–46

Dunand-Sauthier I, Hohl M, Thorel F *et al.* (2005) The spacer region of XPG mediates recruitment to nucleotide excision repair complexes and determines substrate specificity. *J Biol Chem* 280:7030–7

Emmert S, Schneider TD, Khan SG *et al.* (2001) The human XPG gene: gene architecture, alternative splicing and single nucleotide polymorphisms. *Nucleic Acids Res* 29:1443–52

Emmert S, Slor H, Busch DB *et al.* (2002) Relationship of neurologic degeneration to genotype in three xeroderma pigmentosum group G patients. *J Invest Dermatol* 118:972–82

Emmert S, Wetzig T, Imoto K *et al.* (2006) A novel complex insertion/deletion mutation in the XPC DNA repair gene leads to skin cancer in an Iraqi family. *J Invest Dermatol* 126:2542–4

Gary R, Ludwig DL, Cornelius HL *et al.* (1997) The DNA repair endonuclease XPG binds to proliferating cell nuclear antigen (PCNA) and shares sequence elements with the PCNA-binding regions of FEN-1 and cyclin-dependent kinase inhibitor p21. *J Biol Chem* 272:24522–9

Hosfield DJ, Mol CD, Shen B *et al.* (1998) Structure of the DNA repair and replication endonuclease and exonuclease FEN-1: coupling DNA and PCNA binding to FEN-1 activity. *Cell* 95:135–46

Ichihashi M, Fujiwara Y, Uehara Y *et al.* (1985) A mild form of xeroderma pigmentosum assigned to complementation group G and its repair heterogeneity. *J Invest Dermatol* 85:284–7

Ito S, Kuraoka I, Chymkowitch P *et al.* (2007) XPG stabilizes TFIIH, allowing transactivation of nuclear receptors: implications for Cockayne syndrome in XP-G/CS patients. *Mol Cell* 26:231–43

Iyer N, Reagan MS, Wu KJ *et al.* (1996) Interactions involving the human RNA polymerase II transcription/nucleotide excision repair complex TFIIH, the nucleotide excision repair protein XPG, and Cockayne syndrome group B (CSB) protein. *Biochemistry* 35:2157–67

Kleijer WJ, Laugel V, Berneburg M *et al.* (2008) Incidence of DNA repair deficiency disorders in western Europe: xeroderma pigmentosum, Cockayne syndrome and trichothiodystrophy. *DNA Repair (Amst)* 7:744–50

Kraemer KH, Lee MM, Scotto J (1987) Xeroderma pigmentosum. Cutaneous, ocular, and neurologic abnormalities in 830 published cases. *Arch Dermatol* 123:241–50

Lalle P, Nouspikel T, Constantinou A *et al.* (2002) The founding members of xeroderma pigmentosum group G produce XPG protein with severely impaired endonuclease activity. *J Invest Dermatol* 118:344–51

Le MN, Egly JM, Coin F (2010) True lies: the double life of the nucleotide excision repair factors in transcription and DNA repair. *J Nucleic Acids* pii:616342

Masutani C, Kusumoto R, Yamada A *et al.* (1999) The XPV (xeroderma pigmentosum variant) gene encodes human DNA polymerase eta. *Nature* 399:700–4

Moriwaki S, Stefanini M, Lehmann AR *et al.* (1996) DNA repair and ultraviolet mutagenesis in cells from a new patient with xeroderma pigmentosum group G and cockayne syndrome resemble xeroderma pigmentosum cells. *J Invest Dermatol* 107:647–53

Moriwaki S, Takigawa M, Igarashi N *et al.* (2012) Xeroderma pigmentosum complementation group G patient with a novel homozygous missense mutation and no neurological abnormalities. *Exp Dermatol* 21:304–7

Norris PG, Hawk JL, Avery JA *et al.* (1987) Xeroderma pigmentosum complementation group G–report of two cases. *Br J Dermatol* 116:861–6

Nouspikel T, Clarkson SG (1994) Mutations that disable the DNA repair gene XPG in a xeroderma pigmentosum group G patient. *Hum Mol Genet* 3:963–7

Nouspikel T, Lalle P, Leadon SA *et al.* (1997) A common mutational pattern in Cockayne syndrome patients from xeroderma pigmentosum group G: implications for a second XPG function. *Proc Natl Acad Sci USA* 94:3116–21

Oh KS, Imoto K, Boyle J *et al.* (2007) Influence of XPB helicase on recruitment and redistribution of nucleotide excision repair proteins at sites of UV-induced DNA damage. *DNA Repair (Amst)* 6:1359–70

Okinaka RT, Perez-Castro AV, Sena A *et al.* (1997) Heritable genetic alterations in a xeroderma pigmentosum group G/Cockayne syndrome pedigree. *Mutat Res* 385:107–14

Rapin I, Lindenbaum Y, Dickson DW *et al.* (2000) Cockayne syndrome and xeroderma pigmentosum. *Neurology* 55:1442–9

Riedl T, Hanaoka F, Egly JM (2003) The comings and goings of nucleotide excision repair factors on damaged DNA. *EMBO J* 22:5293–303

Scharer OD (2008) Hot topics in DNA repair: the molecular basis for different disease states caused by mutations in TFIIH and XPG. *DNA Repair (Amst)* 7:339–44

Staresincic L, Fagbemi AF, Enzlin JH *et al.* (2009) Coordination of dual incision and repair synthesis in human nucleotide excision repair. *EMBO J* 28:1111–20

Thoms KM, Kuschal C, Oetjen E *et al.* (2011) Cyclosporin A, but not everolimus, inhibits DNA repair mediated by calcineurin: implications for tumorigenesis under immunosuppression. *Exp Dermatol* 20:232–6

Thorel F, Constantinou A, Dunand-Sauthier I *et al.* (2004) Definition of a short region of XPG necessary for TFIIH interaction and stable recruitment to sites of UV damage. *Mol Cell Biol* 24:10670–80

Volker M, Mone MJ, Karmakar P *et al.* (2001) Sequential assembly of the nucleotide excision repair factors in vivo. *Mol Cell* 8:213–24

Yoneda K, Moriue J, Matsuoka Y *et al.* (2007) Xeroderma pigmentosum complementation group G in association with malignant melanoma. *Eur J Dermatol* 17:540–1

Zafeiriou DI, Thorel F, Andreou A *et al.* (2001) Xeroderma pigmentosum group G with severe neurological involvement and features of Cockayne syndrome in infancy. *Pediatr Res* 49:407–12